Bioorganic & Medicinal Chemistry 16 (2008) 8237–8243

Contents lists available at ScienceDirect

Bioorganic & Medicinal Chemistry

journal homepage: www.elsevier.com/locate/bmc

Comparative docking studies of labdane-type diterpenes with forskolin at the active site of adenylyl cyclase

Catherine Koukoulitsa [a,*], Maria Zervou [a], Costas Demetzos [b], Thomas Mavromoustakos [a,c,*]

[a] Institute of Organic and Pharmaceutical Chemistry, National Hellenic Research Foundation, Vas. Constantinou 48, 11635 Athens, Greece
[b] Department of Pharmaceutical Technology, School of Pharmacy, University of Athens, Panepistimiopolis Zografou, 15771 Athens, Greece
[c] Department of Chemistry, University of Athens, Panepistimiopolis Zografou, 15771 Athens, Greece

ARTICLE INFO

Article history:
Received 21 February 2008
Revised 3 July 2008
Accepted 16 July 2008
Available online 26 July 2008

Keywords:
Cistus
Labdane-type diterpenes
Labd-13(*E*)-ene-8a,15-diol
Adenylyl cyclase
Docking
Molecular modeling
2D NMR

ABSTRACT

Diterpen labd-13(*E*)-ene-8a,15-diol (**1**) is a natural product found to possess potential cytotoxic and cytostatic effects against human cancer cell lines. Adenylyl cyclases (ACs) are promising pharmacological targets for treating heart failure, cancer, and psychosis. It has been demonstrated that forskolin is a potent adenylyl cyclase activator. Labdane **1** belongs to same family as forskolin. Its conformational properties are explored using a combination of 1D, 2D NMR spectroscopy, and molecular modeling techniques. The derived low energy conformers are subjected to docking calculations aiming to reveal similarities and differences in the binding mode between **1** and forskolin. Additionally, docking calculations performed on the 1α,9α-OH and 1α-OH derivatives of **1** suggest major contribution of 1α position in increasing binding affinity. This information may be of paramount importance to medicinal chemists who are interested in the synthesis of proposed analogs and test the docking results through *in vitro* experiments.

© 2008 Elsevier Ltd. All rights reserved.

1. Introduction

Labdane-type diterpenes constitute a significant class of natural products. They occur in several plants such as conifers and plants from the genus *Cistus*, and have been reported to exhibit a variety of biological activities such as antialgal, antibacterial, antifungal, antiprotozoal, enzyme inducing, anti-inflammatory, modulation of immune cell functions, as well as cytotoxic and cytostatic effects against leukemic and human tumor cell lines.[1–5] Labdane **1** (Fig. 1) has been investigated for its cytotoxic and cytostatic effect against human cancer cell lines and has proved to be active.[3,6] This compound belongs to the same chemical class as forskolin (**2**) (Fig. 1) and it is found to be a potent adenylyl cyclase activator.[7] For the above reasons, it was suggested that it may have a common mechanism of action.[5]

Forskolin leads to a transient cessation of DNA synthesis.[8] In addition to S phase, forskolin also inhibits progression of cells through other phases of the cell cycle. Forskolin induces cell cycle arrest at $G_{0/1}$ phase in human fibroblasts and B lymphoid cells, and has been reported to cause down regulation of *c-myc* mRNA.[9] Forskolin also induces apoptosis in malignant glioma cells and primary granulose cells via upregulation of the cAMP/PKA pathway.[10,11]

Adenylyl cyclases (ACs) is a family of enzymes that hydrolases ATP to produce pyrophosphate and cAMP, one of the major second messengers that plays an important role in regulation of numerous cellular functions. Elevation of intracellular cAMP levels either stimulates or inhibits proliferation of cells depending on the cell type.[11]

The structural elucidation of **1** (Fig. 1) has been reported elsewhere.[12–13] However, the assignments of proton resonances of its decalin system are described in this study for the first time. Additionally, carbon signals which were not definitely assigned in the past,[14] are unambiguously identified. In the current study, the conformational properties of **1**, using a combination of nuclear magnetic resonance (NMR) spectroscopy and molecular modeling techniques, are explored. In a successive step, docking studies of the derived conformers are performed with the amino acid environment of the forskolin binding site of AC. The aim of this research activity was to investigate its possible binding modes and compare them with forskolin. Structure–activity relationships for activation of adenylyl cyclase by forskolin and its derivatives have demonstrated that derivatization or lack of the 1α- and 9α-hydroxyl functions results in a marked reduction in activity.[15] Thus, it was of great interest to examine the mode of interaction of 1α,9α-OH derivatives of **1** with the amino acid environment of the forskolin binding site of AC.

* Corresponding authors. Tel.: +30 210 7273870; fax: +30 210 7273872 (T.M.).
E-mail addresses: koukoulitsa@eie.gr (C. Koukoulitsa), tmavro@eie.gr (T. Mavromoustakos).

0968-0896/$ - see front matter © 2008 Elsevier Ltd. All rights reserved.
doi:10.1016/j.bmc.2008.07.061

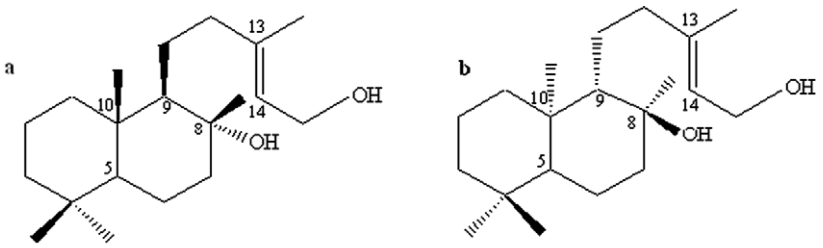

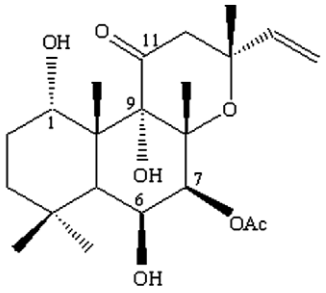

Figure 1. Molecular structures of labd-13(*E*)-ene-8a,15-diol (**1**) and forskolin (**2**).

2. Results and discussion

2.1. Structure elucidation and conformational analysis of labd-13(*E*)-ene-8a,15-diol

The complete assignments of all proton resonances of compound **1** for the first time are achieved (Fig. 2), using a combination of 1D ^{1}H and ^{13}C NMR, and 2D homonuclear and heteronuclear NMR spectroscopy. ^{1}H and ^{13}C chemical shifts are presented in Table 1. ROESY experiments provided valuable information on the spatial proximity between protons of the flexible side chain and those of the decalin system. The most critically observed ROE between decalin proton H1α and one of the 12-CH_2 was subjected to quantification, and the corresponding interatomic distance was found to be 2.5 Å.

X-ray structure of **1**[16] was subjected to molecular dynamic experiments and led to 7 low energy conformers, which are depicted in Figure 3a. The torsion angles of the conformers and their energy values are presented in Table 2. Dihedral τ_1 adopts values around 100° or 160°, while dihedral τ_2 can be *trans* or *gauche* leading to an extended configuration of the alkyl chain (conformers **I**, **II**, **IV**, **V**, and **VI**) or a less extended (conformers **III** and **VII**).

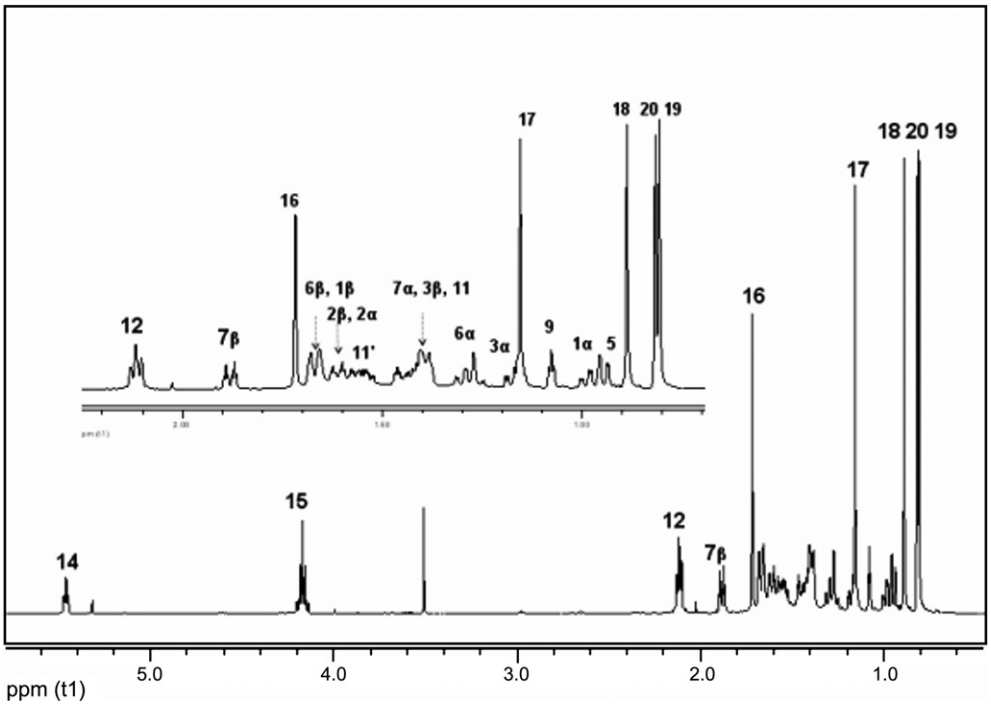

Figure 2. ^{1}H NMR spectrum of **1** in $CDCl_3$ at 298 K recorded on a Varian INOVA 600 MHz.

Table 1
^{1}H and ^{13}C NMR data of labd-13(*E*)-ene-8a,15-diol (**1**) (δ in ppm, *J* in Hz) in $CDCl_3$ at 298 K

Position	δ_H	δ_C
1α,1β [a]	0.98 *dd* (*J* = 3.6, 12.6), 1.65 *br*	39.97
2α,2β	1.59 *t* (*J* = 3.6), 1.60 *t* (*J* = 3.0)	18.66
3α,3β	1.18 *dd* (*J* = 3.6, 13.2), 1.37m	42.20
4		33.46
5	0.94 *dd* (*J* = 1.8, 12.0)	56.34
6α,6β	1.28m, 1.67 *br*	20.79
7α,7β	1.37m, 1.86 *dt* (*J* = 3.0, 12.6)	44.79
8		74.34
9	1.07 *t* (*J* = 4.2)	61.45
10		39.46
11,11′	1.53m, 1.38m	23.81
12,12′	2.12d (*J* = 7.6), 2.11 d (*J* = 8.4)	43.11
13		141.19
14	5.45 *t* (*J* = 7.2)	123.38
15	4.16m	59.53
16	1.71s	16.66
17	1.14s	24.16
18	0.88s	36.60
19	0.80s	21.18
20	0.81s	15.68

[a] α and β are used to designate axial and equatorial positions, respectively.

Table 2
Dihedral angles and energy values of the low energy conformers of **1a** derived from molecular dynamics simulations

Conformer	Energy (Kcal/mol)	τ_1	τ_2	τ_3	τ_4	τ_5
I	9.1	165	−159	79	87	47
II	11.2	167	−161	75	−95	−174
III	11.2	102	87	−154	−22	−175
IV	9.8	105	177	−78	−89	−41
V	13.4	168	−167	162	132	180
VI	10.1	167	−165	160	−88	−34
VII	9.9	158	−69	85	98	174

τ_1: C10–C9–C11–C12, τ_2: C9–C11–C12–C13, τ_3: C11–C12–C13–CH_3, τ_4: C13–C14–C15–O, τ_5: C14–C15–O–H.

The lowest energy conformers **I** and **IV**, which could additionally support the spatial proximity of one of the 12-CH_2 with the decalin proton 1α (±20% of the experimentally derived value), were further subjected to grid scan analysis around torsion angles τ_1 and τ_2, in order to examine more systematically the flexibility of the alkyl chain. The lowest energy levels and those which are higher in energy by as much as 10 Kcal/mol are obtained, while the energy minima are further optimized and led to the conformers **I** (**a**–**d**) and **IV** (**a**–**d**) as shown in Figure 3b and c, respectively. The torsion angles and the energy values of these low energy conformers are presented in Table 3. The *trans* or *gauche* dihedral τ_2 defines an extended arrangement of the alkyl chain (conformers **I (a,b)** and **IV (a,b)**) or a rather vertical arrangement of it in respect to the decalin scaffold (conformers **I** (**c**,**d**) and **IV** (**c**,**d**)). Conformers **I-c** and **IV-d** turn the 12-CH_2 group away from the decalin proton 1a and thus cannot be supported by experimental results. The energetically favorable conformers, which are in agreement with ROE data, adopt for dihedral τ_1 positive values ∼100° (conformers **I** (**b**,**d**) and **IV** (**a**,**c**)) or ∼165° (conformers **I-a**, and **IV-b)**. Among conformers with the extended conformation of the alkyl chain, the negative or positive sign of the dihedral τ_3 defines the orientation of the 16-CH_3 group toward the 8-OH or away from it. Finally, it has to be noted that conformation **I-b** closely resembles that of the X-ray structure as it is depicted from the low RMSD value (RMSD = 6.074 10^{-3}).

The conformational features of the enantiomer **1b** are also investigated, for comparison reasons, by applying the same systematic algorithm around torsion angles τ_1 and τ_2. The obtained lowest energy levels and those which are higher in energy by as much as 10 Kcal/mol. The structures corresponding to the obtained minima after optimization led to the conformers (**a**′–**g**′) as shown in Figure 3d. The respective torsion angles and energy values are

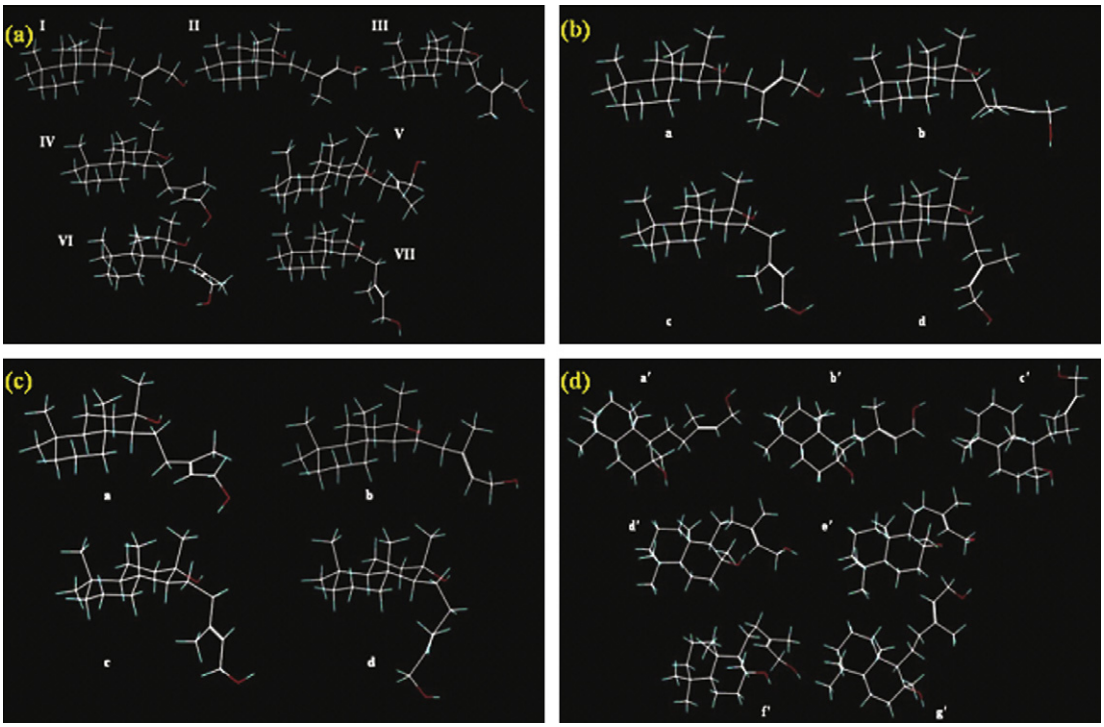

Figure 3. (a) Low energy conformers of **1a** derived from molecular dynamics simulations; (b) low energy conformers of **I** (**a**–**d**); (c) low energy conformers of **IV** (**a**–**d**); and of (d) low energy conformers **a**′–**g**′.

Table 3
Dihedral angles and energy values of the low energy conformers **I** (**a**–**d**) and **IV** (**a**–**d**) of **1a** derived from grid scan search analysis

Conformer	Energy (Kcal/mol)	τ_1	τ_2	τ_3	τ_4	τ_5
I-a	9.1	170	−160	78	87	47
I-b	10.1	107	−172	78	87	46
I-c	8.2	160	−80	77	87	44
I-d	10.2	95	59	72	90	38
IV-a	9.8	105	177	−77	−89	−41
IV-b	10.0	165	−164	−77	−87	−45
IV-c	8.5	102	80	−80	−91	−40
IV-d	10.7	130	−70	−77	−89	−40

τ_1: C10–C9–C11–C12, τ_2: C9–C11–C12–C13, τ_3: C11–C12–C13–CH_3, τ_4: C13–C14–C15–O, τ_5: C14–C15–O–H.

presented in Table 4. The features of the derived conformers resemble those already described for the enantiomer **1a**, namely the extended (conformers **a**′ and **b**′) or less extended (conformers **c**′–**f**′) alkyl chain defined by similar and opposite dihedrals τ_1 and τ_2. Besides, a value of $\tau_1 \sim -130°$ in combination with a gauche(−) dihedral τ_2 favors the spatial proximity between the 15-OH group and the decalin 8-OH (conformers **d**′ and **e**′) and even an intramolecular H-bonding between the two groups leading to an exceptional decrease of the energy (conformer **e**′). Positive values for dihedral τ_1, which position the alkyl chain to the same side of space as the 17, 19, and 20-CH3 groups, lead to conformers with increased energy value (conformer g′), which are not further supported by ROE data.

2.2. Docking studies of receptor–ligand interactions

Nine isoforms of adenylyl cyclase have been identified. With the exception of one, all of them are stimulated by forskolin. They all contain a short cytosolic amino terminus followed by two repeats of six transmembrane helices and a cytosolic domain. Each of the two cytoplasmatic domains, designated as C1 and C2, respectively, is implicated in catalysis. Forskolin binds to the catalytic core at the opposite end of the same ventral cleft that contains the active site and activates the enzyme by gluing together the two cytoplasmic domains in the core (C1 and C2) using a combination of hydrophobic and hydrogen bond interactions.[17]

The X-ray structure of the rat type II adenylyl cyclase C2 domain/forskolin complex (PDB 1ab8)[18] was used in our docking calculations after deletion of the inhibitor forskolin from the PDB file, obtained from the Brookhaven Protein Data Bank.[19] The structure was shown to be a homo dimer containing two molecules of forskolin. The structure indicates that forskolin has polar interactions to both C2 units, that is, 1α-OH and the 11-oxo groups are hydrogen bonded with AspA1018, IleA1019, and GlyA1021, respectively, while 7-acetyl group with SerB942 (Fig. 4a).[18]

Table 4
Dihedral angles and energy values of the low energy conformers **a**′–**g**′ of **1b** derived from grid scan search analysis

Conformer	Energy (Kcal/mol)	τ_1	τ_2	τ_3	τ_4	τ_5
a′	8.0	−167	162	−78	20	178
b′	9.2	−100	175	−78	20	177
c′	9.5	−146	78	−82	20	47
d′	10.6	−133	−90	−77	19	175
e′	4.5	−127	−73	−74	25	47
f′	12.7	−95	−59	−72	15	173
g′	14.4	57	174	−76	19	177

τ_1: C10–C9–C11–C12, τ_2: C9–C11–C12–C13, τ_3: C11–C12–C13–CH_3, τ_4: C13–C14–C15–O, τ_5: C14–C15–O–H.

In order to investigate the location and the structural characteristics of the binding mode of **1** and to compare them with forskolin, docking studies were carried out. Docking calculations were performed using GLUE software implemented in the GRID-22 package.[20]

The crystallographic structure of forskolin docked into AC was used in order to validate the reliability of the docking software. GLUE provided an excellent result since a low value of RMSD (best docked solution of 0.47 Å) was observed between the crystallographic and the calculated docked structure (−8.57 Kcal/mol) (Fig. 4b). This gave confidence that GLUE would exhibit a similar accuracy with the investigated molecule in the current study.

Docking calculations for all conformers derived from the described computational studies of compound **1a** were performed. Since the binding pocket of AC is rather hydrophobic,[22] the predicted binding mode of **1a** may be reasoned by its increased lipophilicity (log*P*: 3.55, calculated by VolSurf program[21,22]). In particular, the docking program positioned **1a** into the pocket of the receptor lying in the same position as that occupied by forskolin (Fig. 5a). The best binding pose, in terms of estimated binding energy, was obtained from docking calculations on conformer **IV-a** (−11.84 Kcal/mol). The molecule is inserted with its side chain in the cavity orienting its decalin system rather vertically compared to the location of forskolin. Furthermore, it establishes mainly van der Waals interactions, which are consistent with those observed for forskolin. More specifically, it fills the hydrophobic pocket consisted of TrpA1020, IleA019, AspA1018, ValA1024, MetA945, PheA889, IleA940, IleB940, PheB895, and LeuB915. Furthermore, the molecule is stabilized by a hydrogen bond forming between the hydrogen of 8-OH group and the crucial amino acid GlyA1021 (OH...O 2.7 Å).

The binding modes of all conformers of **1b** within the forskolin binding site are also analyzed. The most favorable energetical solution (−8.60 Kcal/mol) emerges from docking calculations on conformer **b**′ (Fig. 5b). The molecule enters into the hydrophobic pocket with its side chain at the same orientation as **1a,** while its decalin system adopts a horizontal arrangement similar to forskolin's skeleton. It can be deduced from Figure 5b that **1b** mainly forms van der Waals contacts as it was described for the enantiomer **1a**. It is also worth noting that the molecule is anchored in the hydrophobic pocket via two hydrogen bonds between its 8-OH group and 15-OH with the key amino acids GlyA1021 (OH...O 2.68 Å) and SerB942 (OH...O 2.29 Å), respectively.

Substitution in positions 1α,9α by hydroxyl groups has been performed, and docking simulations have been conducted on the two derivatives of **1** (conformers **IV-a** and **b**′), in order to predict their binding affinity. The docking study revealed decrease in estimated binding energy of 1α,9α-OH derivative of **1a** (−7.82 Kcal/mol) and insignificant difference in the binding energy of 1α,9α-OH derivative of **1b** (−8.32 Kcal/mol). The 1α,9α-OH derivative of **1a** enters in the forskolin binding site with its side chain maintaining the same orientation as forskolin. Despite the reduced binding energy, an interaction with the key amino acid AspA1018 through hydrogen bonding (8-OH...O 2.75 Å) is observed. On the other hand, the 1α,9α-OH derivative of **1b** is inserted in the same mode as **1b**, forming important interactions with IleA1019 and AsnA1025 (8-OH...O 2.57 E, and 1-OH...O2.52 Å) (Fig. 6a and b).

Since 9-hydroxyl group is not absolutely essential for activity,[15] it triggered us to perform docking simulations on 1α-OH derivatives of **1a and 1b**. The estimated binding energy is increased for both of them in respect to **1a** and **1b**. More specifically, the estimated binding energy of 1α-OH derivative of **1a** resulted to be −12.37 Kcal/mol, and that 1α-OH derivative of **1b** equal to −9.88 Kcal/mol. Figure 7a and b illustrate the hydrophobic region in the forskolin binding site with the binding poses of the two derivatives. It is worth to note that the 1α-OH group is involved

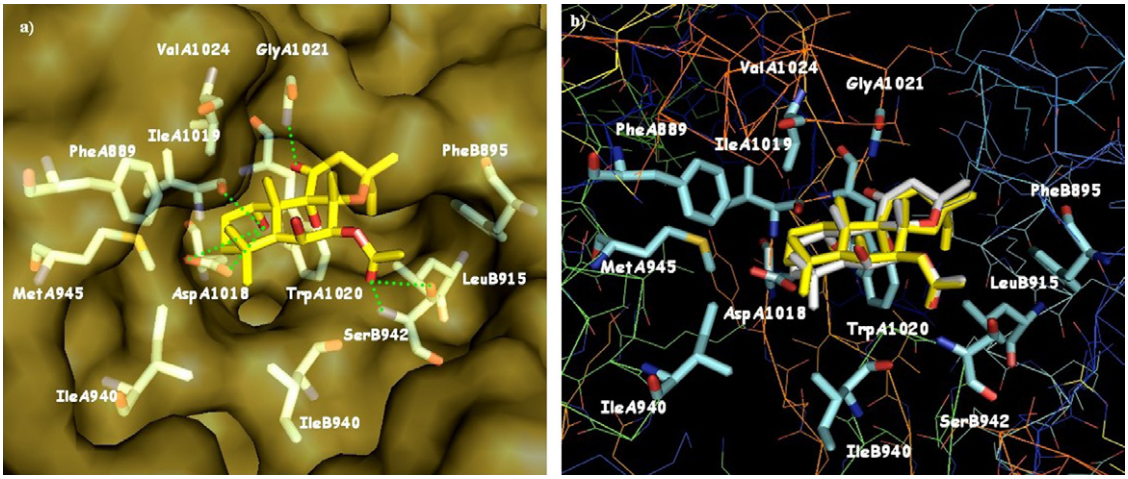

Figure 4. (a) Polar interactions of forskolin and adenylyl cyclase according to Ref. [17]; (b) Conformational comparison between X-ray structure of forskolin (colored by atom type) and predicted (colored yellow) by GLUE.

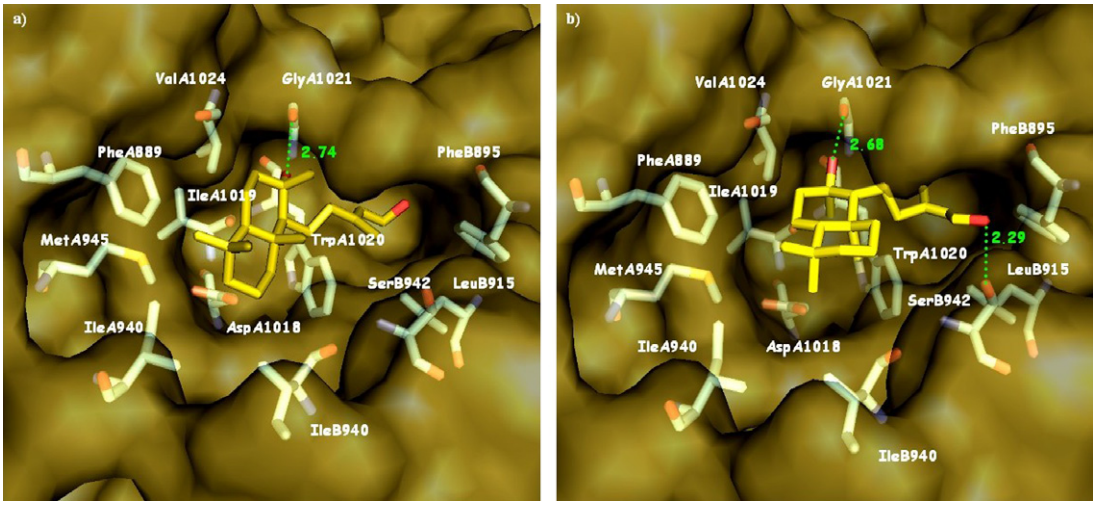

Figure 5. Best binding poses of (a) compound **1a** and (b) compound **1b** in the forskolin binding site of adenylyl cyclase. Hydrogen bonds are depicted as dotted lines.

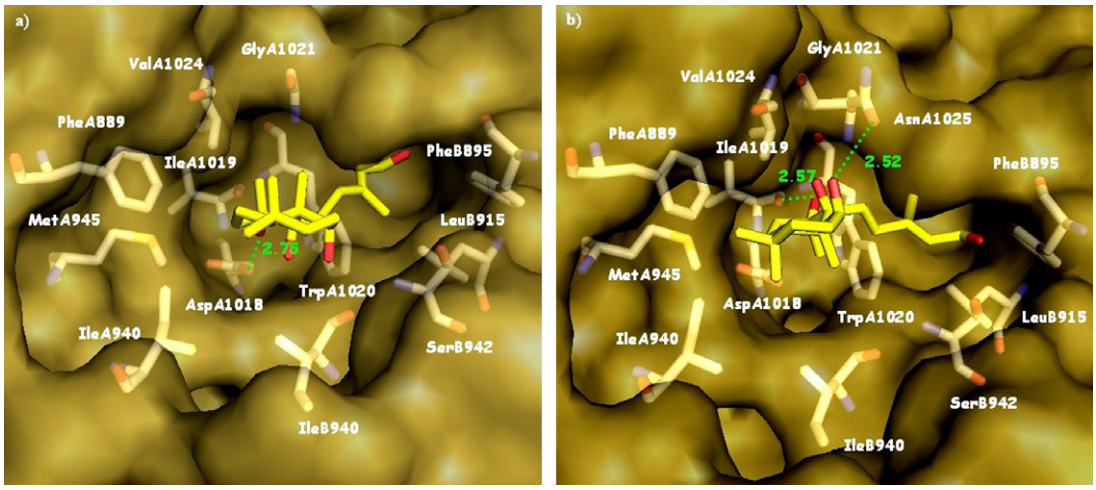

Figure 6. Best binding poses of (a) 1α,9α-OH derivative of **1a** and (b) 1α,9α-OH derivative of **1b** in the forskolin binding site of adenylyl cyclase. Hydrogen bonds are depicted as dotted lines.

in a hydrogen bond with the key amino acid AspA1018 (OH...O 2.46 Å) in the 1α-OH derivative of **1a,** while further stabilization is attributed to a hydrogen bond between 8-OH group and GlyA1021 (OH...O 2.75 Å). Concerning the 1α-OH derivative of

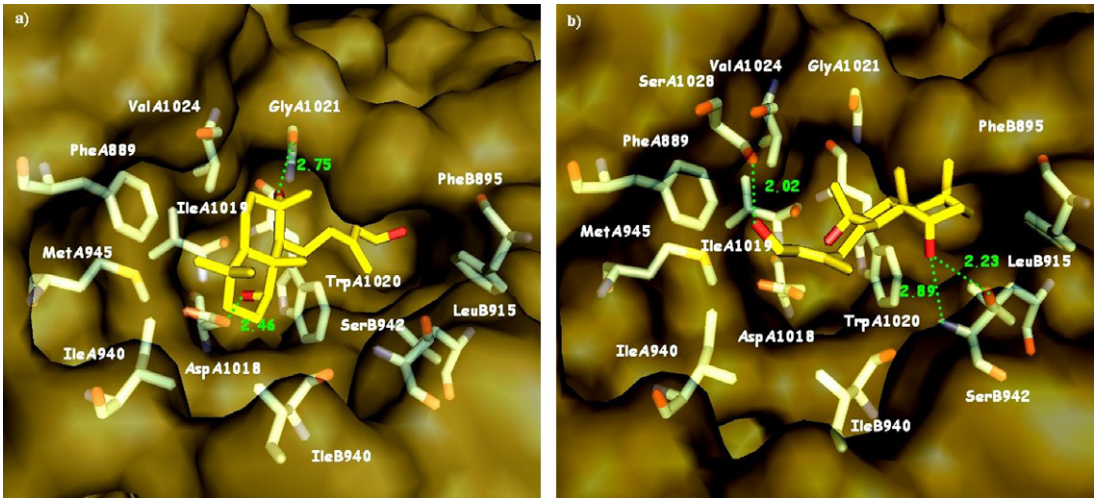

Figure 7. Best binding poses of (a) 1α-OH derivative of **1a** and (b) 1α-OH derivative of **1b** in the forskolin binding site of adenylyl cyclase. Hydrogen bonds are depicted as dotted lines.

1b, two hydrogen bonds between the 1α-OH group and the key amino acid SerB942 (OH...N 2.89 Å, OH...O 2.23 Å) are observed. Moreover, an additional hydrogen bond between 15-OH with SerA1028 (OH...O 2.02 Å) is formed. These findings suggest that substitution by a hydroxyl group in the 1α position of compound **1** is expected to enhance its binding affinity in the forskolin binding site.

3. Experimental

3.1. Isolation of labd-13(*E*)-ene-8a,15-diol (1)

Labd-13(*E*)-ene-8a,15-diol (**1**) (Fig. 1) was isolated from the resin 'Ladano' of the plant *Cistus creticus* subsp. *creticus* that grows in the island of Crete (Greece) (collector Dr. C. Demetzos). Column chromatography for isolating and purifying **1** was performed on silica gel (Merck, 230–400 mesh). Analytical thin layer chromatography (TLC) was carried out on Merck silica gel F254 plates. The method is described elsewhere.[16]

3.2. Nuclear magnetic resonance experiments

$CDCl_3$ (99.96%) and ultra precision NMR tubes Wilmad 535–5 mm (SPINTEC ROTOTEC) were used for the NMR experiments. NMR spectra were recorded on a Varian INOVA 600 MHz and a BRUKER AC 300 MHz spectrometer. The DQF-COSY, ^1H–^{13}C HSQC, and ^1H–^{13}C HMBC were performed with gradients. The ROESY experiments with an optimum mixing time of 300 ms were performed in the phase-sensitive mode. The ^1H spectral window used was 6000 Hz. The homonuclear 2D proton spectra were acquired with 4096 data points in t_2 dimension, 4–32 scans, 256–512 complex points in t_1 dimension and a relaxation delay of 1–1.5 s. The ^{13}C spectral width was 30000 Hz. The ^1H–^{13}C heteronuclear experiments were acquired with 1024–4096 data points in t_2 dimension, 32–64 scans and 128–1024 complex points in t_1 dimension. Experimental data were processed using VNMR or WinNMR routines. Spectra were zero-filled two times and apodized with a squared sine-bell function shifted by $\pi/2$ in both dimensions.

Interatomic proton–proton distances were calculated using the two-spin approximation, and as a distance reference the integrated cross peaks intensity of the geminal H-7α and H-7β protons was assumed to be 1.75 Å. Upper and lower limit constraints were estimated as ±20% of the resulted value.

3.3. Computational methods

3.3.1. Molecular modeling and conformational search

Computer calculations were performed on a Silicon Graphics O2 workstation using QUANTA software purchased from MSI applying the CHARMm energy function and force field. X-ray structure was used as the initial structure.[16] The structure was energy minimized using the steepest descents, conjugate gradient, Powell, Newton–Raphson, and Adopted-Basis Newton–Raphson algorithms with an energy gradient tolerance of 0.001 Kcal/mol Å as convergence criterion. The minimized structure was then subjected to molecular dynamics simulations. The energy minimized structure was heated to 2000 K during a time period of 12 ps with a heating rate of 0.17 K/step and a sampling frequency of 0.01 ps to sample 1200 frames of conformers. The equilibration lasted for 12 ps followed by the simulation process run for 12 ps with a time step of 0.001 ps and a sampling frequency of 0.01 ps. The produced structures were optimized by the steepest descents algorithm with 2000 steps and 0.001 Kcal/mol Å as convergence criterion. Cluster analysis by torsion generated eight structure families [RMSD = 76.96]. The lowest energy representatives of the families were further optimized and finally gave seven different conformers. Grid scan search was performed for two bond rotation around dihedral angles τ_1 and τ_2 in the range 0–360° in steps of 10°. The produced structures were optimized by the steepest descents algorithm with 2000 steps and 0.001 Kcal/mol Å as convergence criterion. Grid torsion angles were constrained during the energy minimization, while subsequent increments were applied to the initial geometry of the structure. All molecular modeling procedures were applied using a dielectric constant $\varepsilon = 1$ to simulate $CDCl_3$ environment.

3.3.2. Docking calculations

Docking calculations were performed with the aid of GLUE program implemented in the GRID package (http://www.moldiscovery.com). GLUE[23,24] is a docking procedure aimed at detecting energetically favorable binding modes of a ligand with respect to the protein active site using the GRID force field.[25] The procedure provides the treatment of ligand flexibility within the protein binding site by means of a 4-point chiral pharmacophoric comparison between the ligand and the site.

The lipophilicity log P was calculated by VolSurf (version 4.1.3, http://www.moldiscovery.com). A PyMOL[26] molecular graphics

system was used in order to visualize the molecules and the results of the docking.

4. Conclusions

In this study, the full assignment of proton resonances of the bioactive labdane **1** is reported for the first time and its conformational properties are studied using a combination of 2D ROESY spectroscopy and molecular modeling techniques. In addition, docking simulations are performed for all conformers of **1a** and **1b**, in the forskolin binding site of adenylyl cyclase. All conformers are placed in the same location as forskolin. The most favorable docked poses reveal mainly hydrophobic interactions with the surrounding residues and hydrogen bonds with crucial amino acids of the forskolin binding site. Furthermore, docking calculations performed on the 1α,9α-OH and 1α-OH derivatives of **1** suggest major contribution of 1α position in increasing binding affinity.

This study aims to trigger the research interest for medicinal chemists to put forward the two major findings of this work. First, it would be desirable to resolve the racemic of **1**, and investigate their cytotoxic and cytostatic effects of the two enantiomers and possibly their effects on adenylyl cyclase-dependent system separately. Second, an effort would be urged for preparation of 1α-substituted analogs of **1** in order to verify the docking results experimentally. We are aware that such an effort may be time consuming, but docking results show that it may be awarded by novel synthetic molecules possessing a better binding affinity to adenyl cyclase system.

Acknowledgments

The authors are grateful to Prof. Gabriele Cruciani (Laboratory for Chemometrics, School of Chemistry, University of Perugia, Italy) for kindly donating the GRID package and the VolSurf program. The authors are also grateful to Dr. Simona Golic Grdadolnic (National Institute of Chemistry, Ljubljana, Slovenia) for the acquisition of the NMR spectra on the INOVA 600 MHz spectrometer through the Bilateral Scientific and Technological collaboration between Greece-Slovenia EPAN-M.4.3.6.1 (2003–2005). Finally, the authors thank Dr. Aris Terzis and Dr. Catherine Raptopoulou (X-ray Laboratory, NCSR 'Demokritos', Greece) for providing the X-ray structure of compound **1**. Catherine Koukoulitsa completed this research activity while she was a recipient of IKY (State Scholarships Foundation).

References and notes

1. Demetzos, C.; Dimas, K. *Stud. Nat. Prod. Chem.* **2001**, *25*, 235.
2. Jung, M.; Ko, I.; Lee, S.; Choi, S. J.; Youn, B. H.; Kim, S. K. *Bioorg. Med. Chem. Lett.* **1998**, *8*, 3295.
3. Dimas, K.; Demetzos, C.; Marsellos, M.; Sotiriadou, R.; Malamas, M.; Kokkinopoulos, D. *Planta Med.* **1998**, *64*, 208.
4. Tanaka, R.; Ohtsu, H.; Iwamoto, M.; Minami, T.; Harukuni, T.; Nishino, H.; Matsunaga, S.; Yoshitake, A. *Carr. Cancer Lett.* **2000**, *161*, 165.
5. Dimas, K.; Demetzos, C.; Vaos, V.; Ioannidis, P.; Trangas, T. *Leuk. Res.* **2001**, *25*, 449.
6. Demetzos, C.; Dimas, K.; Hatziantoniou, S.; Anastasaki, T.; Angelopoulou, D. *Planta Med.* **2001**, *67*, 614.
7. Seamon, K. B.; Padgett, W.; Daly, J. W. *Proc. Natl. Acad. Sci. U.S.A.* **1981**, *78*, 3363.
8. Naderi, S.; Wang, J. Y. I.; Chen, Tung-Ti.; Gutzkow, K. B.; Blomhoff, H. K. *Mol. Biol. Cell* **2005**, *16*, 1527.
9. Heldin, N. E.; Paulsson, Y.; Forsberg, K.; Heldin, C. H.; Westermark, B. *J. Cell Physiol.* **1989**, *138*, 17.
10. Keren-Tal, I.; Such, B. S.; Dantes, A.; Lindner, S.; Oren, M.; Amsterdam, A. *Exp. Cell Res.* **1995**, *218*, 283.
11. Chen, T. C.; Hinton, D. R.; Zidovetzki, R.; Hofman, F. M. *Lab Invest.* **1998**, *78*, 165.
12. Galabuig, M. T.; Cortıs, M.; Francisco, C. G.; Hernαndez, R.; Suαrez, E. *Phytochemistry* **1981**, *20*, 2255.
13. Demetzos, C.; Harvala, C.; Philianos, S. M. *J. Nat. Prod.* **1990**, *53*, 1365.
14. Forster, P. G.; Ghisalberti, E. L.; Jefferies, P. R. *Phytochemistry* **1985**, *24*, 2991.
15. Seamon, K. B.; Daly, J. W.; Metzger, H.; Souza, N. J.; Reden, J. *J. Med. Chem.* **1983**, *26*, 436.
16. Matsingou, C.; Hatziantoniou, S.; Georgopoulos, A.; Dimas, K.; Terzis, A.; Demetzos, C. *Chem. Phys. Lipids* **2005**, *138*, 1.
17. Onda, T.; Hashimoto, Y.; Nagai, M.; Kuramochi, H.; Saito, S.; Yamazaki, H.; Toya, Y.; Sakai, I.; Homcy, C. J.; Nishikawa, K.; Ishikawa, Y. *J. Biol. Chem.* **2001**, *276*, 47785.
18. Zhang, G.; Liu, Y.; Ruoho, A. E.; Hurley, J. H. *Nature* **1997**, *386*, 247.
19. RCSB Protein Data Bank, operated by the Research Collaboratory for Structural Bioinformatics.
20. GRID version 22, Molecular Discovery Ltd, 4. Chandos Street, W1A 3BQ, London, United Kingdom.
21. VolSurf is available from Molecular Discovery Ltd., 4. Chandos Street, W1A 3BQ, London. United Kingdom.
22. Cruciani, G.; Pastor, M.; Guba, W. *Eur. J. Pharm. Sci.* **2000**, *11*(Suppl. 2), S29.
23. Carosati, E.; Sciabola, S.; Cruciani, G. *J. Med. Chem.* **2004**, *47*, 5114.
24. Sciabola, S.; Carosati, E.; Baroni, M.; Mannhold, R. *J. Med. Chem.* **2005**, *48*, 3756.
25. Goodford, P. J. *J. Med. Chem.* **1985**, *28*, 849.
26. *The PyMOL Molecular Graphics System. DeLano Scientific*; DeLano, W. L., Ed.; San Carlos: CA, 2002.